



Ratchet Analysis of Piping Systems by Dynamic Elasto-Plastic FEM

Nobuyoshi Iriki¹⁾, Toshiaki Hisada²⁾, Hiroshi Watanabe²⁾, Tetsundo Nakatogawa³⁾ and Koichiro Oketani¹⁾

1) Kobe Shipyard & Machinery Works, Mitsubishi Heavy Industries, Ltd., Japan

2) The University of Tokyo, Japan

3) Obayashi Corporation, Japan

ABSTRACT

The current seismic design of a piping system for nuclear power plants are being based on the elasticity analysis on a principle. Therefore, as a reasonable seismic design approach for the future, research is progressing in a direction admitted the accepted and/or controlled plastic deformation in which a piping system doesn't lead to failure. On the other hands, when postulated seismic loads for design become stronger, we must check the safety margin. However, it is difficult to conduct many dynamic tests to investigate the behavior of an actual piping system, and we require the FEM code that can investigate dynamic behavior accurately.

For these above reasons, taking into account the effects of ratcheting, we have developed the elasto-plastic FEM code that can analyze the dynamic behavior of a piping system.

1. Introduction

The current seismic design for nuclear power plants are being based on elasticity analysis as a principle. Against this background, as a reasonable seismic design approach for the future, research is progressing in a permissible direction based on the analysis of material plastic deformation. From this viewpoint, it is particularly important to estimate the limited response behaviors of structures at the time of a large earthquake, in order to ensure safety and reliability.

In our research, we are handling seismic piping design as one application field toward the actual implementation of such a design approach. In this case, an analysis method with a good accuracy is important, but with the finite element analysis code (i.e., program) at present, the dynamic elasto-plastic FEM analysis of 3D piping systems including even the ratchet phenomenon (described below) lies in difficult circumstances.

Ratchet is a phenomenon in which, for example, local plastic strain accumulates on the part of piping systems due to the cyclic loading. When ratchet occurs in an actual piping system, cracks appear from the locations of occurrence, and there are many cases of failure. Because of this, designs are being done in accordance with safety margin with seismic design standards.

The objective of the present research lies in the development of an analysis method that will make dynamic 3D piping system simulation possible for ratchet behavior. For this purpose, in the piping system as a whole, we use elasto-plastic elements at locations considered safe from the ratchet (because the strain at these locations is comparatively smaller), and elasto-plastic solid elements with nonlinear geometric characteristics at locations considered susceptible to the ratchet, and perform analysis by combining the both of them. In addition, we perform an actual dynamic elasto-plastic analysis on a piping system, and investigate the relationship between the piping system pressure and ratchet as well as the effect local ratchet has on the total response of the piping system.

2. Outline of the Dynamic Elasto-plastic FE Analysis

2.1 Formalization of elasto-plastic solids

In this research the elasto-plastic constitutive equation is derived based on the assumptions of associated flow rule, the isotropic and kinematic hardening and von Mises yield function.

$$\text{Von Mises equivalent stress} \quad \bar{\sigma} = \left(\frac{3}{2} \bar{\sigma}'_i \bar{\sigma}'_i \right)^{\frac{1}{2}} \quad (1)$$

$$\text{Yield function} \quad F = \bar{\sigma} - S_y \quad (2)$$

$$\text{Associated flow rule} \quad \dot{\epsilon}^p_{ij} = \dot{\lambda} \frac{\partial F}{\partial \sigma_{ij}} \quad (3)$$

$$\text{Prager evolution law} \quad \dot{\alpha}_{ij} = C \dot{\lambda} \frac{\partial F}{\partial \sigma_{ij}} = C \dot{\epsilon}^p_{ij} \quad (4)$$

As an extension of this classical elasto-plastic constitutive equation to finite deformation, our research takes following approach. If it is considered that the velocity vector v of a material point is given by the sum of the elastic component v^e and plastic component v^p , i.e. $v = v^e + v^p$, it is easy to see that decomposition according to $D = D^e + D^p$ is established even with a deformation rate tensor D obtained from the symmetric components of a velocity

gradient tensor \mathbf{L} . So the plastic strain rate \dot{e}^p_{ij} used in the associated flow rule and Prager evolution law is changed to D^p_{ij} . If the Jaumann rate of the relative Kirchhoff stress is used for the objective stress rate in the virtual work equation of rate form due to the updated Lagrangian method, we have a symmetric tangential stiffness matrix used in the finite element method.

2.2 Formulation of pipe element

In this research, the four-node isoparametric pipe element developed by Bathe and co-workers (1)~(4) is utilized. The coordinate axes and the stress components in an pipe element are shown in Fig.1. The basic assumptions of this element are as follows:

- (1) The plane normal to the central axis remains flat although it is no longer normal to the axis after the deformation.
- (2) The circumferential strain $e_{\xi\xi}$ is zero at points halfway between the inner and outer radii and the $\xi\eta$ -plane is under a plane stress condition.

With the notation in Fig.1, strains $(e_{\xi\xi})_{ov}$, $(e_{\eta\eta})_{ov}$, and $(e_{\eta\xi})_{ov}$ are derived as follows.

$$(e_{\xi\xi})_{ov} = \frac{1}{\alpha^2} \left(\frac{\partial \omega_\xi}{\partial \phi} + \frac{\partial^3 \omega_\xi}{\partial \phi^3} \right) \zeta \quad (5)$$

$$(e_{\eta\eta})_{ov} = \frac{1}{R - \alpha \cos \phi} \left(\omega_\xi \sin \phi + \frac{\partial \omega_\xi}{\partial \phi} \cos \phi \right) - \left(\frac{1}{R - \alpha \cos \phi} \right)^2 \frac{\partial^2 \omega_\zeta}{\partial \theta^2} \zeta \quad (6)$$

$$(e_{\eta\xi})_{ov} = \frac{1}{R - \alpha \cos \phi} \frac{\partial \omega_\zeta}{\partial \theta} \quad (7)$$

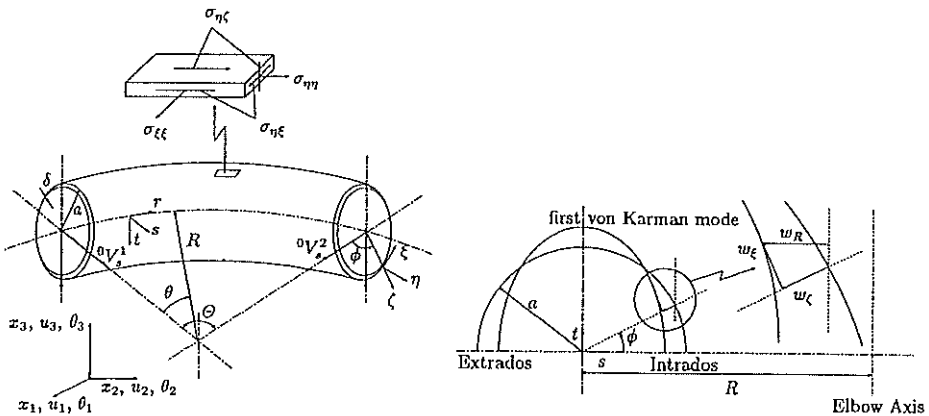


Fig.1 Coordinate system and displacement of pipe elements.

2.3 Formulation of the dynamic combination analysis

The dynamic virtual work equation of rate form due to the updated Lagrangian method with a constraint condition $\chi(t'u) = 0$ at time $t' = (t + \Delta t)$ based upon the penalty method is given as follows.

$$\int_V \rho_v \dot{u}^i \delta u^i dv + \int_V \dot{S}^i : \delta \epsilon^i E dv - \int_s \dot{f}^i \cdot \delta u^i ds - \int_V \rho_v \dot{g}^i \delta u^i dv + \int_\Omega \alpha \chi \cdot \delta \chi d\Omega = 0 \quad (8)$$

Here, ρ_v , \dot{S}^i , $\dot{\epsilon}^i$, \dot{f}^i , and $\rho_v \dot{g}^i$ shows the mass density, the relative second Piola-Kirchhoff stress, the relative Green-Lagrange strain, the surface force and the body force, α shows the penalty parameter and Ω is domain the constraint condition is given.

In this research, to combine the above-mentioned elasto-plastic solid elements and pipe elements, constraint function χ is constructed such that a material point of the pipe element that agrees with the nodal coordinate of solid element in the state before the state of deformation also agrees after the deformation. .

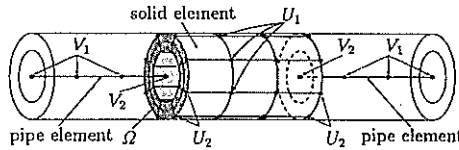


Fig. 2 Pipe-solid combination model.

3. Analysis Example

3.1 Analysis model

The analysis model assuming piping of radius 89.1mm and a thickness of 5mm (3B Sch 40) with two areas of bending on the piping. The material was stainless steel (SUS304TP, equivalent SA312TP304) seamless piping. However, only one of the areas of bending has an inner thickness of 3mm (3B Sch 10S) for the purpose of limiting the occurrence locations of ratchet. Fig. 3 and Fig. 4 shows the dimension data.

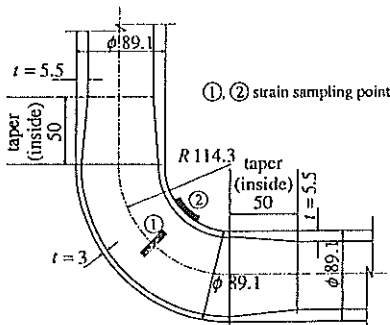


Fig.3 Dimensions of ratchet elbow.

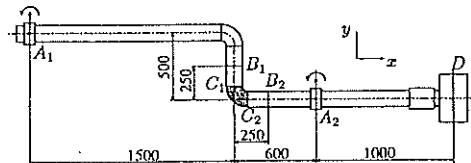


Fig.4 Piping system under in-plane vibration.

The piping system used in the vibration experiment are one-axis rotation-free supports (the other degrees of freedom are restricted) at the locations shown by A_1 and A_2 in Fig. 4, and a weight of 200kg is added to terminal D. By loading an internal pressure of 100kgf/cm² (9.8 MPa, S_m equivalent) to produce stress equivalent to the allowable stress S_m to the piping system, A_1 and A_2 are given a y-axis sine wave acceleration input. In the present analyses, the frequency of the input acceleration is 5 Hz and the acceleration is 1910 gal (19.1 m/sec²).

For the internal pressure, we performed analyses for four values: 0 kgf/cm² (0 Pa), 50 kgf/cm² (4.9 MPa, $S_m/2$ equivalent), 81 kgf/cm² (7.938 MPa, the actual value in the experiment), and 100 kgf/cm² (9.8 MPa, S_m equivalent) for the purpose of comparison. The time step of the dynamic analysis is $\Delta t = 0.0002$ seconds; the dynamic analysis is carried out during vibration for 20 seconds, 100 times. In addition, the Newmark- β method without iteration ($\beta = 1/6$, $\gamma = 1/2$) is employed for the time integration, and there is no repetition calculation. The conventional forward Euler method is used for the stress integration in the elasto-plastic analysis. Rayleigh damping is employed for the damping factor, with coefficient of mass matrix and stiffness matrix, 1.385 and 7.316×10^{-4} respectively.

The stainless steel material used in the experiment has a Young's modulus of 21,000 kgf/mm² (205.8 GPa), a Poisson ratio of 0.3, and a yield stress of 25 kgf/mm² (245 MPa). In the case, curve fitting to stress-plastic strain curve was carried out by n-power law. In addition, we hypothesize the isotropic hardening and the kinematic hardening in the analysis example presented, and compare the results.

3.2 Analysis results

Fig. 5 and Fig. 6 each shows the strain history of a location (1: circumferential direction or 2: longitudinal direction, respectively) shown in Fig. 3 for vibration of 20 seconds at an internal pressure of 100 kgf/cm² (9.8 MPa). The strains at these parts are oscillated and increase (or decrease) according to the progression of the ratchet.

In the current analysis, the displacements and even the responses of the strains become somewhat like sine waves because the given input includes the acceleration of sine waves. All of the graphs below approximate the strain histories with the equation $a \sin(x) + b$, and display the strain histories of a and b .

Below, a is called the amplitude of the strain and b is called the mean strain. A result shown by com. (i.e., combination) with a marker in the figure is a result obtained by the combination analysis, and a result shown by i (i.e., isotropic hardening) or k (i.e., kinematic hardening) is a result obtained under isotropic hardening or kinematic hardening.

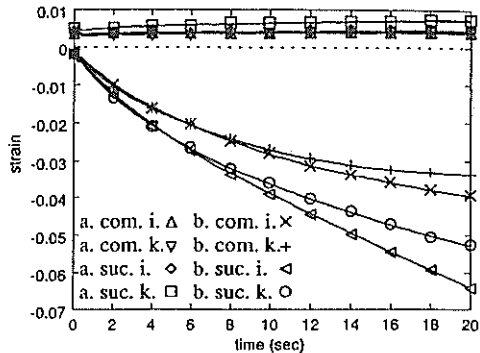
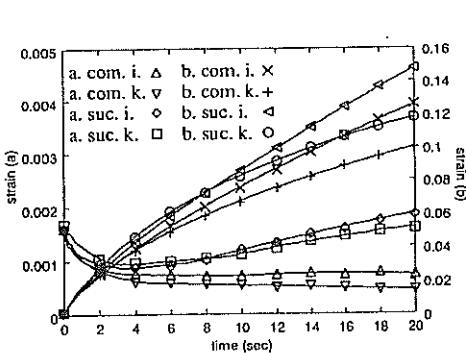


Fig. 5 Strain history at sampling point 1. Fig. 6 Strain history at sampling point 2.

From the view point of practical utilization, if the stiffness of the piping system as a whole does not change significantly by the progress of the ratchet, the analysis can be carried out only by the pipe elements first. Then, the displacements of both terminals at the elbow part are calculated from the obtained transformation, amount of rotation, and cross-section deformation coefficients. Next, by using the displacements as a input of the elasto-plastic solid elements, a detailed analysis can be carried out by the successive approximation analysis. Here, we call this "successive analysis".

A detailed explanation of the analysis procedure is omitted here, but results obtained through successive analyses on ratchet elbow are included in Fig. 5 and Fig. 6. The results are shown as suc. (successive) at the markers in the figures. As shown in these figures, both do not agree with the current analysis model.

Fig. 7 shows ratchet elbow deformations. In the figure (and in subsequent figures), the opening on the right side is B_1 , and that on the left side is B_2 . The displacements are magnified three times to facilitate reader understanding. In addition, the white parts in the figure are elements yielded more than one time. Regardless of the case (i.e., isotropic hardening or kinematic hardening), the bent piping is flattened and large deformations are observed locally.

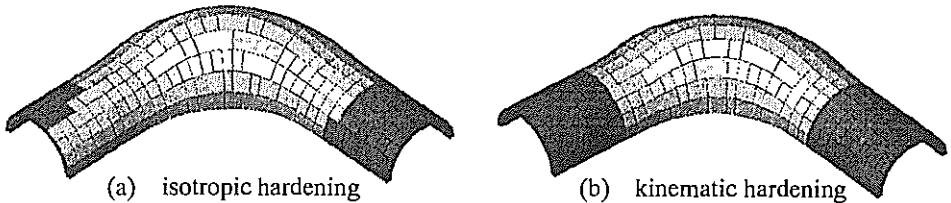


Fig. 7 Deformation and plastic region at $t = 20$.

Concerning the development condition of the plastic region, almost the whole body of the ratchet elbow (between $C1-C2$) yields within one cycle in the same way regardless of the internal pressure. After this, results are obtained indicating the gradual development of the plastic region to both sides, toward $B1$ and $B2$.

As one example, Fig. 8 shows the development condition for a plastic region under isotropic hardening and an internal pressure of 100 kgf/cm^2 (9.8 MPa). It can be understood that the development of the plastic region goes up to the neighborhoods of the taper portions on both sides of the elbow.

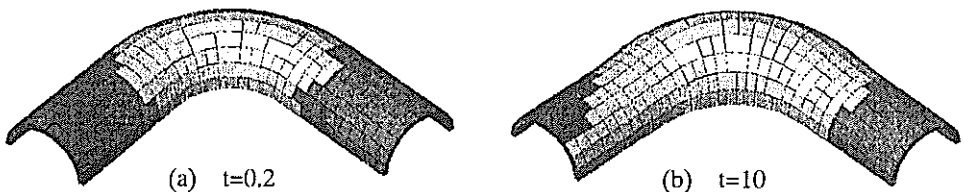


Fig. 8 Deformation and plastic region.

As is well known, unless the internal pressure works, ratchet does not occur. As one example of a comparison between the internal pressure and the growth rate of ratchet, Fig. 9 shows the histories of strains in the circumferential direction under isotropic hardening. The

values stipulated to the sides of the markers indicate the internal pressures. It can be seen that the internal pressure and the growth rate of the mean strain are roughly proportional. In addition, Fig. 10 shows deformation under isotropic hardening after vibration for 20 seconds under internal pressure loads of 0 kgf/cm² (0 Pa) and 50 kgf/cm² (4.9 MPa).

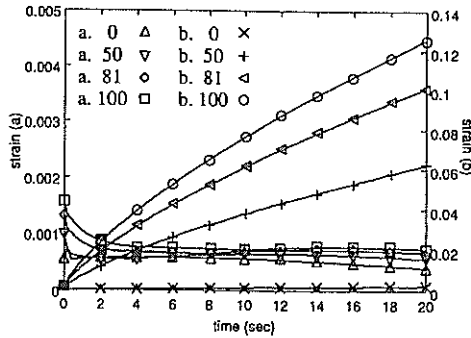


Fig. 9 Strain history at sampling point 1.

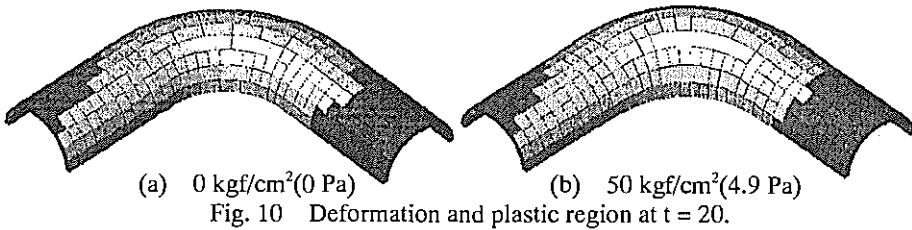


Fig. 10 Deformation and plastic region at $t = 20$.

As explained above, the strain histories of the combination analysis and successive analysis do not agree. Fig. 11 shows a comparison of the y-direction displacements of weights obtained in analyses involving the combination analysis and only pipe elements. Here, the internal pressure is 100 kgf/cm² (9.8 MPa).

As can be understood from this figure, when analysis is carried out with pipe elements, the weight vibrates at nearly fixed locations, while there is movement with the combination analysis. Looking at this finding from a wide perspective, a transformation mode seems to emerge causing the ratchet.

This would explain why the combination analysis on the amplitude of strain in the circumferential direction in Fig. 5 maintains a fixed value, while an increase is observed with the successive analysis. It can be considered that the combination analysis on the average strain in the longitudinal direction in Fig. 6 makes the progression speed slower, while a linear change is observed with the successive analysis. However, although a difference exists in the construction principles concerning the mean strain speed in the circumferential direction, we do not recognize differences in the analysis methods. With the elasto-plastic analysis, the weight vibrates centering on the origin.

In addition, Fig. 12 shows results investigating the effect of the internal pressure on the y-direction displacement of the weight. For the analysis with only the pipe elements, the internal pressure has no effect and there is vibration centering on the same fixed locations, but for the combination analysis, the displacements increase following increases in the

internal pressure. Even when the internal pressure is 0 kgf/cm², the effect (e.g., the above-mentioned warping) on the deformation of the elbow part can be considered large (because the displacements of both models differ). We believe that the above finding provides a valuable clue for the development of future pipe elements.

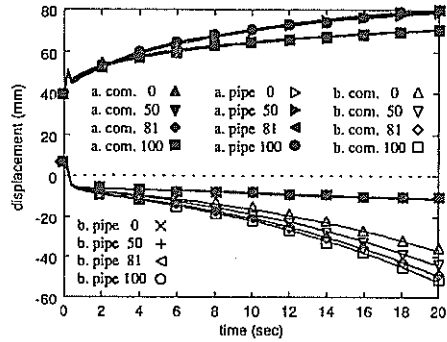
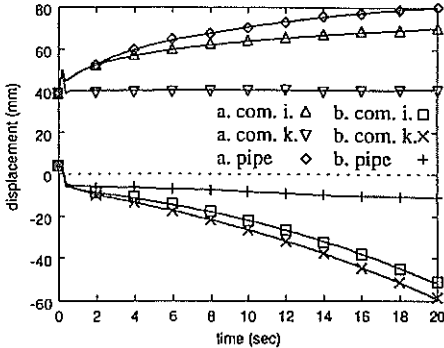


Fig. 11 Deformation history of the weight

Fig. 12 Deformation history of the weight

4. Conclusion

We have developed a dynamic elasto-plastic piping - solid combination analysis code making dynamic response simulation possible on 3D piping systems with ratchet. In addition, we have performed an actual dynamic analysis on a piping system, and have confirmed that the phenomenon of local ratchet, can be simulated accurately in the case of a combination analysis reproduced in analysis involving only pipe elements but instead requires a high-accuracy analysis involving a combination analysis.

References

1. Bathe, K. J. and Almedia, C. A., ASME J. Appl. Mech, Vol. 47, 93, 1980.
2. Bathe, K. J. and Almedia, C. A., *ibid*, Vol. 49, 165, 1982.
3. Bathe, K. J. and Almedia, C. A., *ibid*, Vol. 49, 914, 1982.
4. Bathe, K. J., Almedia, C. A. and Ho, L. W., Comput. Struct., Vol. 17, 659, 1983.
5. Benson, D. J. and Hallquist, J. O., Int. J. Num. Meth. Eng., Vol. 12, 723, 1986.
6. Park, K. C. and Saczalski, K. J., Trans. ASME, J. Eng. Ind., Vol. 96, 1041, 1974.
7. Tong, P. and Rossetos, J. N., Comput. Struct., Vol. 7, 109, 1977.
8. Belytschko, T., Schwer, L. and Klein, M. J., Int. J. Num. Meth. Eng., Vol. 11, 65, 1977.
9. Kleiber, M. and Rojek, J., Proc. Structural Mechanics in Engineering, Vol. 2, 1, 1994.
10. Fujita, Shiraki, Kitade and Nakamura, Kiron, 44-386, 3437, 1978.